A Quantitative Study of the Interactions between Organic Functionalities and the Surface of Silver Nanoparticles in Aqueous Systems

An essay submitted in partial fulfillment of

the requirements for graduation from the

Honors College at the College of Charleston

with a of Bachelor of Science in

Chemistry

Sondrica Goines

May 2018

Advisor: Katherine M. Mullaugh, PhD

Table of Contents

Abstract

As nanoparticles become increasingly commonplace in many consumer products, the release of nanomaterials into natural waters is inevitable and potentially harmful. Silver nanoparticles (Ag NPs), the most widely used type of nanomaterial, is of special concern due to the toxicity of silver to many aquatic organisms. Recent laboratory studies examining the behavior of Ag NPs in various conditions have demonstrated the importance of nanoparticle surface chemistry in the potential transformations of Ag NPs such as dissolution and aggregation. However, specific interactions between Ag NPs and organic compounds are usually not quantified. Furthermore, most studies to date have used large, poorly characterized natural organic material (NOM) standards, making it difficult to achieve a molecular-level understanding of relevant NOM-NP interactions that control NP behavior. We have investigated a method by which Ag NPs are allowed to react with various organic compounds and, following a size-based separation, the amount of compound that remains unadsorbed is determined by HPLC or voltammetry. Preliminary results indicate adsorption of benzoic acid derivatives bearing carboxylate groups are negligible under the conditions examined, but adsorption of thiol derivatives was significant. The extent of adsorption varied based on the adsorbate molecule as well as the separation method used, ultrafiltration or centrifugation. Additionally, the sensitivity for thiols with voltammetry allowed for experiments at lower, more environmentally relevant concentrations. Complementary SERS spectra were used to provide a qualitative understanding of the interactions between various organic functionalities and the surface of Ag NPs in aqueous systems, and UV-vis spectra provided evidence of adsorbate induced NP dissolution and aggregation.

Introduction

Nanocrystals are typically defined as crystals with at least one dimension between 1 and 100 nm, and viewed as the intermediate between atoms and bulk materials.[1] The unique properties of matter on the nanoscale, combined with advances in nanotechnology have resulted in a large increase in the use of nanomaterials in consumer goods.[2] Of the nanomaterials found in consumer products, silver nanoparticles (Ag NPs) are the most common due to their antimicrobial properties and high reactivity, which is a consequence of their high relative surface area. The use of Ag NPs in medical fields continues to rise as the NPs are implemented in the struggle against anti-biotic resistant bacteria.[3] The antimicrobial properties of Ag NPs also make them useful in other goods such as toys, clothing, and personal care and cleaning products.[4] Therefore, release of Ag NPs into the environment is inevitable and due to their large surface area to mass unit ratio they are potential binding agents for organic and inorganic materials in aqueous systems.[5] Despite the widespread use of Ag NPs, there is limited knowledge concerning the environmental effects of nanosilver. The unique properties of Ag NPs as well as the complexity of organic matrices in natural waters present challenges to designing a method for an analytical assessment of the interactions between Ag NPs and natural organic material (NOM) in aqueous systems.
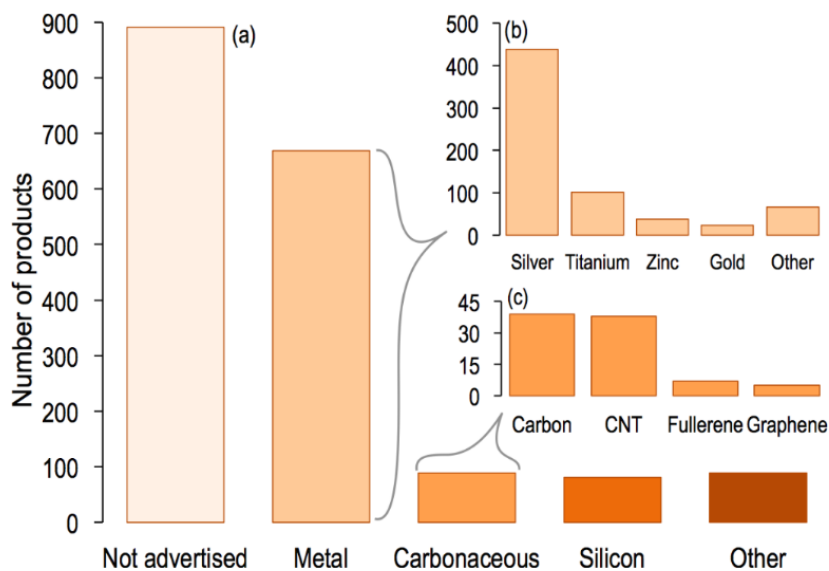
Figure 1. (a) Claimed number of nanomaterials listed in the CPI, grouped into five major categories. (b) Claimed number of nanomaterials listed based on elemental composition according metal components. (c) Claimed number of carbonaceous nanomaterials. [2]

The first initiative to understand the extent to which nanomaterials are used in consumer products was the creation of the Nanotechnology Consumer Product Inventory (CPI) in 2005 produced by the Woodrow Wilson International Center for Scholars and the Project on Emerging Nanotechnology. With just five years (2005–2015), the list grew from 54 products to 1,012 products from companies around the world (Figure 1).[2] As the number of products continue to grow, regulatory agencies have been geared towards gathering information concerning the environmental effects of nanomaterials.[5] Although nanomaterials can form naturally in the environment, the increased use of nanomaterials, particularly those containing toxic metals like silver, can result in abnormal quantities of nanoparticles or their component elements in various environments.[5, 6] For instance, nanoparticles that are used in the production of sunscreens, cosmetics, and paints are loosely bound and may easily enter surface waters or soil when consumers use and dispose of these products.[5, 6] Nanomaterials, such as Ag NPs, may also be introduced to the environment in the form of waste from industrial facilities.[5]

Studies focusing on the environmental transformations of Ag NPs have stated that Ag NPs are toxic to many aquatic organisms such as plants, algae, and fungi due to the release of Ag^+ ions following the oxidative dissolution of the Ag NPs in aqueous environments.[7] Ironically, the toxicity of Ag NPs that allows them to be utilized in antimicrobial pathways also makes the particles
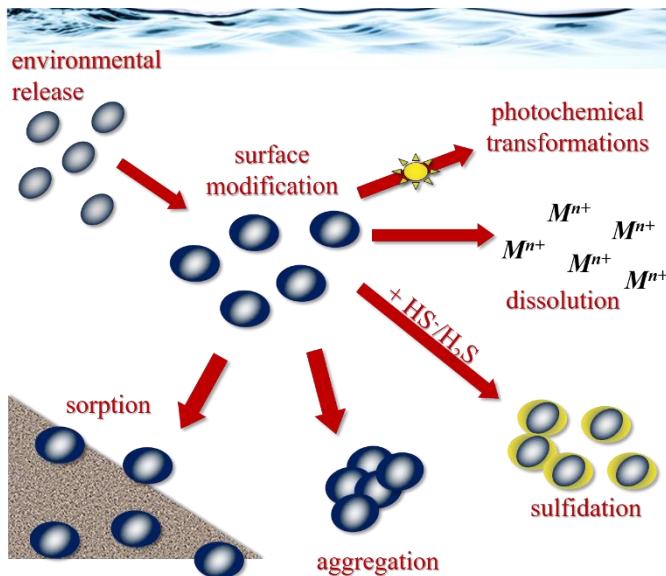

Figure 2. Potential chemical and physical transformations of silver nanoparticles in natural aqueous environments. Prepared by Dr. Katherine M. Mullaugh.

potentially harmful to organisms in natural waters.[4, 8] The goal of the following research project is to use laboratory-based studies to determine the physical and chemical changes Ag NPs may undergo in aqueous systems in order to better understand their fate in aquatic environments.

Of all the various changes nanoparticles can undergo in aqueous conditions, one of the most important yet poorly understood is the various surface modifications that can occur post-release. It is expected that changes to Ag NP surface chemistry will affect subsequent changes such as oxidative dissolution, aggregation, and sorption of nanoparticles onto other surfaces (Figure 2).[7] Like most metal nanocrystals, Ag NPs are generally produced with an organic capping agent such as polyvinyl pyrrolidone or citrate.[6, 9] Following release into aquatic environments, the capping agents of nanosilver may be completely or partially exchanged with natural organic material (NOM) such as humic acid and fulvic acid.[9] Recent laboratory experiments have shown that interactions between humic material and Ag NPs may affect the surface characteristics of nanoparticles, which would in turn affect the fate of the particles in aqueous environments.[10]

Adsorption of humic material onto the surface of Ag NPs may affect the nanoparticles' tendency to aggregate, dissolve in solution, or adsorb to surrounding surfaces in the aqueous phase.[11] For example, cysteine has been observed forming a thiol protective barrier on the surface of the Ag NPs resulting in reduced antimicrobial activity of the particles due to inhibition of dissolution.[12] Therefore, there are surface modifications of Ag NPs that may either promote or inhibit Ag NP dissolution, but present research does not offer a detailed understanding of the extent to which these modifications occur and the relative importance of the organic functionalities that are bound to the surface of Ag NPs.[4, 12] For example, despite their low abundance thiols can control metal speciation in many aquatic systems.[13]

To gain a more detailed understanding of the interactions between NOM and the surface of Ag NPs, the following research project will quantify the adsorption of organic compounds onto the surface of Ag NPs by using small molecules selected based on the functional groups within humic material such as carboxylate, amine, hydroxyl, and thiol functionalities. By utilizing small molecules rather than large, poorly characterized natural organic molecules such as humic acid, the project will avoid the difficulties associated with the inherent complexity of NOM (Figure 3).[14] Bypassing the use of NOM like humic acid avoids the practical difficulties in separating the macromolecular NOM from similarly sized NPs; a small molecule approach may also provide definitive information concerning the role of specific functionalities in the adsorption process. Ag NPs will be allowed to react with various small organic compounds, and following a size-based separation, the amount of
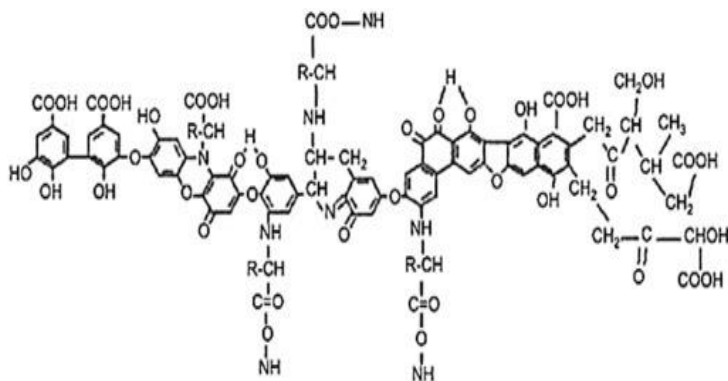

Figure 3. Proposed chemical structure of humic material.[14]

7

compound that remains unabsorbed will be determined by UV-vis spectroscopy, HPLC, or voltammetry (Figure 4).
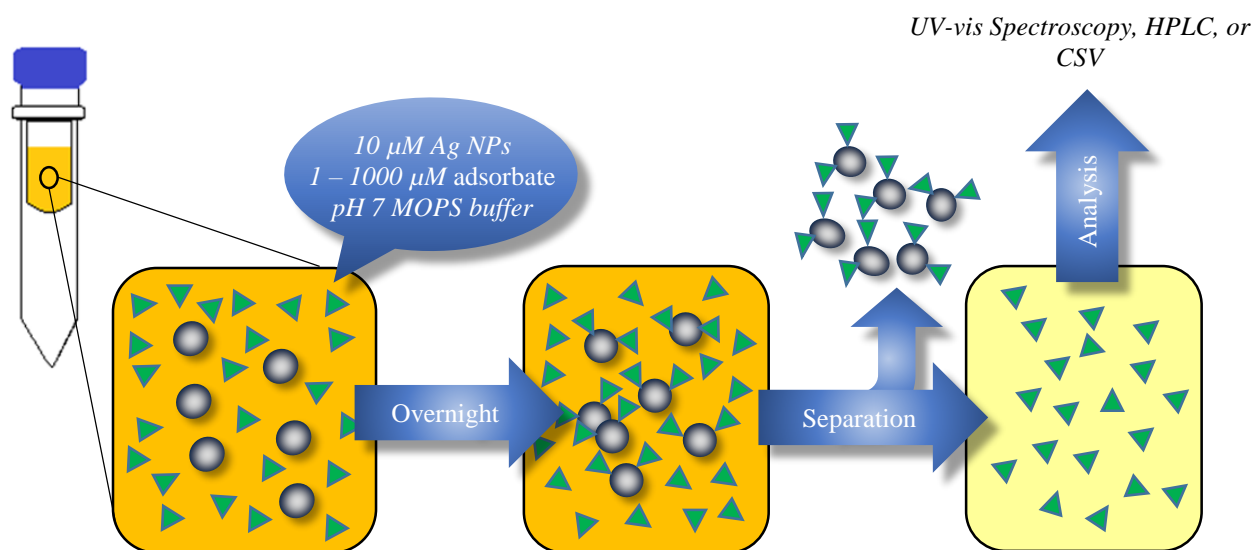

Figure 4. Schematic of the experimental approach to study the adsorption of organic material onto the surface of Ag NPs.

The method of detection of the unadsorbed fraction will be amended based on the sensitivity of the instrument in relation to the adsorbate material being studied. Adsorption experiments were carried out in a pH 7 MOPs buffer to simulate environmental conditions within a laboratory setting. Within samples a known amount of adsorbate material and Ag NPs were combined. By using adsorbate molecules such as phthalic acid, 4-aminobenzoic acid, and 4-mercaptobenzoic acid adsorption experiments could be used to determine the role of specific functionalities in complexation reactions between NOM and the surface of Ag NPs. Additionally, this experimental design allowed for size-based separation via ultrafiltration or centrifugation that would be otherwise impossible if similarly, sized NOM, such as humic acid, were used in combination with Ag NPs. Following separation, the filtrates were analyzed using various modes of analysis depending on the functionalities of the adsorbate used.

UV-vis and HPLC

To gain a quantitative understanding of the extent to which adsorption occurs, UV-vis spectroscopy may be utilized to detect the quantity of unabsorbed material following adsorption experiments. UV-vis spectroscopy allows for immediate discrimination between Ag NPs and organic material in solution because the spherical Ag NPs used in this study typically absorb light in the visible region at approximately 400 nm, while the aromatic compounds used in adsorption experiments typically absorb light in the UV region. Due to the immediate discernment between Ag NPs and the adsorbates in solution, conclusions may be made concerning the efficacy of the Ag NP separation (ultrafiltration or centrifugation). Following separation, removal of Ag NPs can be confirmed by a loss of the peak at 400 nm indicative of Ag NPs in solution. Utilizing long path length (10 cm) cells can improve sensitivity, but the effect of pH on the molar adsorptivity of adsorbate compounds presents challenges for quantification. Therefore, reverse phase High Performance Liquid Chromatography (HLPC) with UV-vis detection was used for the quantification of unabsorbed organic material following adsorption experiments. The use of liquid chromatography allows for detection of the unadsorbed benzene derivatives at an absorbance wavelength specific to the derivative following chromatographic separation. Consequently, the chromatographic separation utilized in HPLC analysis provides greater sensitivity and pH-control, which allows for experiments at more environmentally relevant concentrations and better reproducibility.[15] The presence of thiol functionalities bound to the benzene derivatives introduces new complexities to the HPLC analysis method due to the potential for thiol oxidation, which requires derivatization of the compounds before HPLC analysis. The addition of this experimental parameter initiated the use of two separate analytical detection methods based on the structure of adsorbate compounds.

Cathodic Stripping Voltammetry

While reversed phase HPLC may be used to detect non-thiol benzene derivatives, cathodic stripping voltammetry (CSV) may be used to detect thiols in solution utilizing a Hanging Mercury Drop Electrode (HMDE). Stripping voltammetry relies on the adsorption of an analyte in solution onto the surface of an electrode.[16] CSV utilizing a HMDE is ideal for thiol detection because thiol functionalities are known to form complexes at the surface of the Hg drop that acts as the working electrode (1).[13] Following a short (<60 sec) accumulation step, CSV allows for simple, sub-μM detection of thiols in solution.[17] After the thiol accumulates on the surface of the drop, cathodic determination of the thiol occurs upon reduction of the mercury(II) thiolate complexes formed on the surface of the Hg drop during accumulation (1).[16]

$$Hg(SR)_2 + 2H^+ + 2e^- \rightarrow 2HSR + Hg \qquad (1)$$

A platinum wire served as the counter electrode and the reference electrode was Ag/AgCl. All potentials reported are vs. Ag/AgCl.

Surface Enhanced Raman Scattering

In addition to gaining a quantitative understanding of the interactions between NOM and the surface of Ag NPs, a qualitative understanding of changes in the Ag NP surface chemistry will be gained using Surface Enhanced Raman Scattering (SERS). Although Raman signals are typically weak, molecules at the surface of various metals, including silver, experience an enhancement of their scattering. The electromagnetic enhancement is the result of the electromagnetic field of a metal surface extending 20 nm above the surface enhancing the signal of nearby molecules, making SERS ideal for adsorption experiments.[18] Additional sensitivity can be gained using metal nanostructures of a particular size, shape, and spacing due to their surface plasmon resonance (SPR) in which the incident photons resonant with the oscillation frequency of

conducting electrons on the metal surface.[19] Recently, SERS has become very useful in environmental studies concerning metal nanocrystals because it is an effective method of detection for analytes near the surface of nanomaterials due to its high sensitivity, specificity, and non-destructive nature.[18, 19] Raman is also an ideal method of qualitative analysis in environmental studies concerning aquatic environments because water is Raman silent. Therefore, SERS may be used to determine the organic functionalities responsible for interactions on the surface of Ag NPs in aqueous systems. In addition to highlighting the functionalities present on the surface of Ag NPs, SERS may also denote the orientation of binding of organic compounds on the surface.[20]

The general experimental approach designed for this project focused on preparing a quantitative method for determining the extent to which adsorption occurs on the surface of Ag NPs. Various factors play a role in the affinity of NOM to the surface of Ag NPs such as the functionalities available for binding to the surface of the nanomaterial, the orientation of the adsorbate material, and the oxidative state of the organic material as well as the silver in solution. This project explores the roles of these properties through quantitative analysis using UV-vis spectroscopy, reversed phase HPLC, and cathodic stripping voltammetry. Additionally, the experimental approach provides a complementary qualitative analysis through SERS that confirms adsorption as an interaction between Ag NPs and organic material in aqueous systems.

Experimental

Materials

All compounds were commercial grade and used without further purification. Table 1 lists adsorbate molecules used along with the manufacturers of the reagents. Additional reagents are listed in Table 2 along with the manufacturers of the reagents. Distilled or deionized milli-q water (resistivity >18.2 MΩ) was used for all solution preparations.

Table 1. List of adsorbate molecules and the manufacturers used in this report, with associated pK_a values.[21]
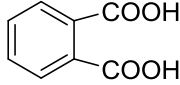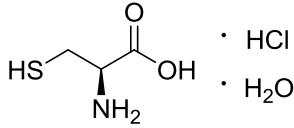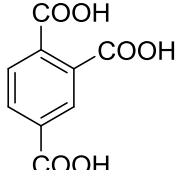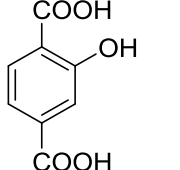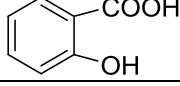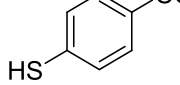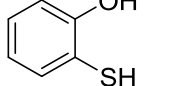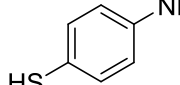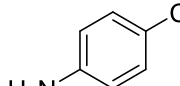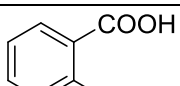
Reagent	Manufacturer	Structure	pK_a values
Phthalic acid (PA)	Alfa Aesar		2.950 5.408
L-cysteine hydrochloride monohydrate (L-cys)	Alfa Aesar		1.7 (COOH) 8.36 (SH) 10.74 (NH$_3$)
Trimellitic acid (TMA)	Tokyo Chemical Industry Co., LTD		2.86 4.30 6.28
4-hydroxyisophthalic acid (4-HIPA)	Tokyo Chemical Industry Co., LTD		N/A
Salicylic acid (SA)	Sigma-Aldrich		2.972 (CO$_2$H) 13.7 (OH)
4-mercaptobenzoic acid (4-MBA)	Acros Organics		N/A
2-mercaptophenol (2-MPN)	Sigma-Aldrich		N/A
4-aminothiophenol (4-ATP)	Alfa Aesar		N/A
4-aminobenzoic acid (4-ABA)	Acros Organics		2.08 (CO$_2$H) 4.96 (NH$_3$)
Thiosalicylic acid (TSA)	Alfa Aesar		N/A

Table 2. List of reagents and the manufacturers used in this report.

Reagent	Manufacturer
Sodium citrate dihydrate	BDH®
Silver nitrate	BDH®
Sodium phosphate monobasic	BDH®
Ultra-pure MOPs	AMERCO
Ultra-pure TRIS	MP Biomedicals, LLC
Potassium nitrate	Alfa Aesar
Manufactured Ag NPs	Alfa Aesar

Instrumentation

The pH of buffers and analytes were determined using a pH electrode (Mettler Toledo SevenExcellence), which was calibrated prior to each use with pH 4,7, and 10 buffers (BDH®). UV/vis spectra were determined using a Cary 60 UV/vis produced by Agilent Technologies (Model No. G6860A). The cells used for UV-vis spectroscopy were 1 cm (quartz) and 10 cm (plastic, $\lambda > 400$ nm). Separation via ultrafiltration was completed using Pall Corporation Microsep™ Advance Centrifugal Devices (3K). Separation via centrifugation was completed using 50 mL Thermo Scientific™ Nalgene™ Centrifuge Ware. HPLC data was obtained using an Agilent 1220 HPLC system with variable wavelength detection. Cathodic Stripping Voltammetry data was collected using a CGME Basi Controlled Growth Mercury Electrode connected to an Epsilon computing device (Model No. E2) from Bioanalytical Systems, Inc. Surface Enhanced Raman Scattering data was collected using an AGILTRON Peak Seeker™ (Model No. PEK-785). Centrifugation experiments were carried out using centrifuges produced by Thermo Scientific: a Sorvall Legend X1 centrifuge (Model No. 75004221) and a Sorvall Lynx 4000 centrifuge (Model No. 75006580).

pH Dependence of Absorbance of Adsorbates

Experiments to study the pH dependence of the detection were carried out using the aromatic compounds: trimellitic acid (TMA), 4-hydroxyisophthalic acid (4-HIPA), phthalic acid

(PA), salicylic acid (SA), and 4-mercaptobenzoic acid (4-MBA) (Table 1). To study the pH dependence of TMA, a 50 μM solution was prepared in an unbuffered solution and the pH was adjusted using HCl or NaOH solutions. After each pH adjustment, the absorbance of the solution was recorded in a 1-cm quartz cell. This pH dependence experimental procedure was repeated for 4-HIPA, PA, SA, and 4-MBA listed in Table 1.

Preparation of Ag NPs Stock Solution

Initially, the Ag NPs utilized in this project were synthesized in the lab. A 500 mL volumetric flask was charged with 5 mL 16 mM $AgNO_3$, 6.25 mL 60 mM Sodium Citrate Dihydrate, and distilled water. The $AgNO_3$/citrate solution was placed in a beaker and 10 mL of 100 mM $NaBH_4$ was added to the solution dropwise while stirring resulting in an immediate change in color to yellow. The contents of the beaker were stirred for 30 minutes. After stirring the solution and conditioning the a 3kDa ultrafiltration disc (Millipore) with distilled water in a cell (Model 8400) while stirring under 40 psi of N_2 gas (UHP purity), approximately 250 mL of the solution is syringe filtered (0.22 μm pore size) into the cell to remove aggregates or large NPs formed prior to ultrafiltration under 40 psi of N_2 gas. After 50% of the solution in the cell was filtered down, and the remaining $AgNO_3$/citrate solution was syringe filtered into to the cell. Once the contents of the cell were filtered back down, 200 mL 0.35 mM Sodium Citrate Dihydrate was added to the cell (2×) to rinse the solution. Following the citrate rinse, two ~50 mL solutions of Ag NPs were prepared. The resulting NP solutions were stored in the dark at 4℃.[22] Lastly, analysis by Flame Atomic Absorption Spectroscopy (FAAS) was completed to determine the concentration of the resulting Ag NP stock solutions. TEM analysis of Ag NPs prepared in this manner were found to be <10 nm in diameter with relatively high polydispersity.[23] Later experiments were

performed with manufactured 20-nm diameter Ag NPs (Alfa Aesar), which aided in reproducibility due to the more monodisperse nature of commercially produced Ag NPs.

Adsorption/Ultrafiltration Experiments Utilizing UV-vis spectroscopy

Following the determination of the optimal pH ranges for UV-vis detection, adsorption experiments were carried out (Figure 5). Buffers for experiments were chosen based on optimal pH ranges for absorbance readings of the organic compound in use. A procedure utilizing the adsorbate trimellitic acid (TMA) follows.

Standard TMA solutions with concentrations ranging from 5 μM to 80 μM were prepared in 25 mL volumetric flasks using 10 mM trimellitic acid and a ~0.1 M phosphate buffer (pH ~2). UV-vis spectra of the standards were recorded to generate a calibration curve.
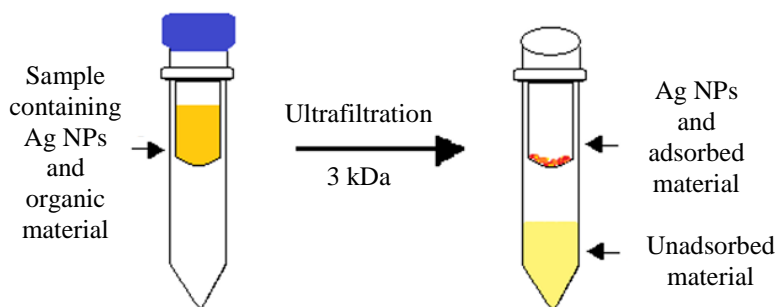

Figure 5. Adsorption/ultrafiltration experimental design.

Following the production of a TMA calibration curve, eight sample solutions were prepared using 1 mM TMA, a pH 7 0.01 M MOPs buffer, and a 1.5 mM Ag NPs stock solution. Four controls ranging from 10 μM to 80 μM TMA were prepared with MOPs buffer and 1 mM TMA. Four additional samples were prepared with the Ag NPs stock to produce complementary solutions of TMA. After each sample was produced, the samples were sonicated for 30 minutes. Following sonication, 3.5 mL of each sample was placed in an ultrafiltration device with a pore size of about 1 to 2 nm (3 kDa). Ultrafiltration of the samples was completed by placing the

ultrafiltration devices in a centrifuge for 10 minutes at 7500 × G speed. During ultrafiltration, the absorbance spectra for the remaining unfiltered samples were recorded after adjusting the pH of the samples from approximately 7 to 2 with an HCl solution. Following ultrafiltration, the pH of the filtered samples was adjusted, and the absorbance spectra of the filtrates were recorded. The adsorption/ultrafiltration experiment was repeated, but the samples were sonicated for 30 minutes and allowed to equilibrate over a 2-hour period rather than completing ultrafiltration immediately after sonication. A similar experiment was carried out with the organic compound, 4-hydroxyisophthalic acid (4-HIPA) in a pH 12.53 ~1 M phosphate buffer due to the pH dependence of the absorbance of 4-HPA.

Adsorption/Ultrafiltration Experiments Utilizing UV-vis spectroscopy: Increasing Ag NPs Concentration

Rather than increasing the concentration of the adsorbate material, the concentration of Ag NPs was increased in the following experiment for comparison purposes. The following experiment utilized 4-hydroxyiosphthalic acid (4-HIPA).

Initially, a 100 µM solution of 4-HIPA in pH 7 0.01 M MOPs buffer was prepared. Eight sample solutions were prepared using the 4-HIPA stock solution and a 1.5 mM Ag NPs stock. Duplicate 10 mL samples of 100 µM Ag NPs, 250 µM Ag NPs, and 500 µM Ag NPs in 100 µM 4-HIPA were prepared, along with two 10 mL controls of 100 µM 4-HIPA.

Following the preparation of the samples, the samples were sonicated for 30 minutes. Ultrafiltration devices (3 kDa) were filled with 3.5 mL of each sonicated sample, and samples were ultrafiltered for 10 minutes at 7500 × G speed. During ultrafiltration, the absorbance spectra for the remaining unfiltered samples were recorded after adjusting the pH of the samples from approximately 7 to 12 using phosphate buffer. Following ultrafiltration, the pH of the filtered

17

samples was adjusted to 12 and the absorbance spectra of the filtrates were recorded. The adsorption/ultrafiltration experiment was repeated, but the samples were sonicated for 30 minutes and allowed to equilibrate over a 3-hour period rather than completing ultrafiltration immediately after sonication to extend the possible adsorption period. Remaining unfiltered samples were kept overnight, and the ultrafiltration procedure was repeated using used ultrafiltration devices that had been soaking overnight in distilled water.

Adsorption/Ultrafiltration Experiments Utilizing HPLC

Accuracy of data collected by UV-vis spectroscopy was not sufficient to infer adsorption of organic compounds by Ag NPs in solution. High Performance Liquid Chromatography (HPLC) offers a more precise detection method for adsorption experiments, therefore parallel adsorption/ultrafiltration experiments were carried out using HPLC. Organic molecules used in adsorption/ultrafiltration experiments in which HPLC was used as the detection method were primarily 4-aminobenzoic acid (4-ABA), phthalic acid (PA), trimellitic acid (TMA), and salicylic acid (SA) (Figure S1-4).

To carry out the 4-ABA adsorption experiment, eight samples were made up using pH 7.01 100 mM MOPs, 0.566 mM Ag NPs stock, 10 mM 4-aminobenzoic acid, 0.35 mM citrate, and distilled water to prepare duplicate samples of 0 µM Ag NPs, 113 µM Ag NPs, 170 µM Ag NPs, and 226 µM Ag NPs.

After preparing the samples, the samples were sonicated for 30 minutes. During sonication, 25 mL standard solutions of ranging from 5 µM to 50 µM 4-ABA were prepared using 10 mM 4-ABA and 0.01 M MOPs. The sonicated samples were allowed to equilibrate over a period of approximately 2.5 hours. Following equilibration, 3.5 mL of each sample was placed in an ultrafiltration device with a pore size of about 1 to 2 nm (3 kDa) and ultrafiltered in a centrifuge

for 10 minutes at 7500 × G speed. After filtration, a portion of each filtrate and standard were placed in labeled HPLC vials for analysis. Uniform HPLC parameters were used for each adsorbate material except for the detection wavelength (Table 3).

Parallel adsorption/ultrafiltration experiments were also carried out with phthalic acid (PA), trimellitic acid (TMA), and salicylic acid (SA) using HPLC as a detection method to compare the extent of adsorption due to the presence of various functionalities such as carboxylate, amine, and hydroxyl groups.

Table 3. HPLC parameters for 4-aminobenzoic acid (4-ABA), phthalic acid (PA), trimellitic acid (TMA), and salicylic acid (SA) adsorption/ultrafiltration experiments.

HPLC Parameters	
Detection λ	4-ABA: 284 nm PA: 235 nm TMA: 240 nm SA: 235 nm
Stationary Phase	ODS HYPERSIL 150 × 4.6 mm Particle Sz. (μ) 5
Mobile Phase	50% 20 mM Formate Buffer pH 3.0 50% Methanol
Injection Volume	20.00 μL
Flow rate	1.000 mL/min

Adsorption of Thiols Experiments Utilizing Voltammetry

Preliminary L-cysteine titration experiments were completed using cathodic stripping voltammetry on the Hanging Mercury Drop Electrode (HMDE). Titration experiments were carried out with various potassium nitrate/buffer electrolyte solutions with varying pH values. Optimal detection of the thiol was carried out using a 0.1 M KNO_3/ 0.01 M TRIS (pH ~8) electrolyte solution.

To carry out experiments, 10 μM L-cysteine was placed in 10 mL of an electrolyte solution in the cell of the HMDE. Following an initial scan of the L-cysteine solution, the solution was

titrated with 100 μM Ag NPs. For comparison purposes, the titration experiment was repeated with

approximately 100 μM AgNO$_3$.

To complete L-cysteine adsorption experiments, eight samples were made up using the

same experimental procedure as used in HPLC adsorption/ultrafiltration experiments. To prepare

samples, volumes of pH 7.01 100 mM MOPs, 0.188 mM Ag NPs stock, 10 mM L-cysteine, 0.35

mM citrate, and distilled water were combined in 15 mL centrifuge tubes. Samples were sonicated

for 30 minutes and given an equilibration period of approximately 2.5 hours. Following

equilibration, the samples were ultrafiltered and analyzed using cathodic stripping voltammetry

(Table 4, Figures S5-6). An additional L-cysteine experiment was completed with 100 mM TRIS

(pH ~8) to prepare samples to observe how pH affects adsorption. Complementary experiments

were completed with 4-MBA (Table 4).

Table 4. Cathodic Stripping Voltammetry parameters for L-cysteine and 4-mercaptobenzoic acid (4-MBA) adsorption/ultrafiltration experiments.

Parameter	L-cysteine	4-MBA
Deposition Time (sec)	20	40
Quiet Time (sec)	5	5
Initial E	Deposition E	Deposition E
Initial Potential (mV)	125	125
Final Potential (mV)	-1300	-1300
Step E (mV)	6	6
S. W. Amplitude (mV)	25	25
S. W. Frequency (Hz)	100	50
Full Scale (+/-)	10 μA	10 μA

Adsorption Confirmation Studies Using Thiols

To confirm that an interaction occurs between the surface of the manufactured Ag NPs and

the thiol, rather than silver cations that may be in solution due to dissolution, silver nitrate was

titrated with 4-mercaptobenzoic acid (4-MBA) following the titration of manufactured 20-nm Ag

NPs with 4-MBA using cathodic stripping voltammetry as an *in-situ* analysis technique. Initially,

a calibration curve was prepared using 4-MBA. Following the preparation of the calibration curve,

a solution of approximately 0.91 µM 4-MBA was titrated with 100 µM Ag NPs (20-nm) until the thiol was essentially undetectable. This procedure was repeated using approximately 100 µM AgNO₃.

Adsorption Experiments Utilizing Centrifugation Separation Method: Increasing Adsorbate Concentration

Poor recovery results following the use of ultrafiltration to separate unabsorbed material from Ag NPs and adsorbed material prompted separation by centrifugation. Following the preparation of 250 µM stock solutions of the thiols 2-mercaptophenol (2-MPN) and 4-aminothiophenol (4-ATP) in purged water, samples for the absorption experiment were prepared in 15 mL centrifuge tubes. The samples were prepared using the 250 µM stock solutions, 160 µM manufactured 20-nm Ag NPs, and 10 mM MOPs buffer (pH ~7). The concentrations of the samples ranged from 1 µM to 20 µM thiol with 10 µM Ag NPs in each sample. The samples were sonicated for 30 minutes and allowed to equilibrate overnight. The following day, approximately 10 mL of each sample was placed in a 50 mL centrifuge tube suitable for centrifugation above 8,000 × G speed. The samples were centrifuged at 21,000 × G at 22 ℃ for 1 hour. Immediately following centrifugation, the supernatant was removed from the centrifuge tube and analyzed using the UV-vis spectrometer to confirm the removal of Ag NPs from unabsorbed material (Figure 6). After UV-vis analysis of the supernatants, the supernatants were analyzed using cathodic stripping voltammetry to determine the concentration of the remaining organic material (Table 5, Figures S7-8). A complementary experiment was carried out using the thiol 4-MBA to correlate the data from experiments with 2-MPN and 4-ATP to previous findings.

Table 5. Cathodic Stripping Voltammetry parameters for 2-mercaptophenol (2-MPN) and 4-aminothiophenol (4-ATP) adsorption/ultrafiltration experiments.

Parameter	2-MPN	4-ATP
Deposition Time (sec)	0	0
Quiet Time (sec)	5	5
Initial E	Deposition E	Deposition E
Initial Potential (mV)	75	100
Final Potential (mV)	-1300	-1400
Step E (mV)	10	40
S. W. Amplitude (mV)	50	25
S. W. Frequency (Hz)	200	100
Full Scale (+/-)	10 μA	10 μA

Qualitative Analysis of Adsorption of Thiols Using SERS

Surface Enhanced Raman Scattering (SERS) was used to confirm the presence of the thiol 4-mercaptobenzoic acid (4-MBA) on the surface of Ag NPs in solution, and therefore to confirm adsorption. Samples were prepared using 1 mM 4-MBA, 160 μM Ag NPs (20-nm), and water to produce samples ranging from 0.35 mM 4-MBA to 0.70 mM 4-MBA with ~50 μM Ag NPs in each sample. Following sample preparation, the samples were sonicated for 20 minutes and analyzed by Raman spectroscopy within a 1-cm quartz cuvette. The samples were analyzed with a laser λ of 785 nm with a 60 second integration time. Spectra of samples were compared to those of a 4-MBA control containing no Ag NPs and an Ag NPs control containing no 4-MBA.

Results and Discussion

To quantify the amount of organic material adsorbed onto to the surface of Ag NPs, an efficient method of detection of the organic compounds in solution was necessary. UV-vis spectroscopy is a detection method for Ag NPs in solution. Synthesized Ag NPs result in a yellow solution that is detected by the UV-vis spectrometer at approximately 400 nm, while solutions of organic compounds utilized in the lab generally resulted in colorless solutions that would be detected at shorter wavelengths. Therefore, UV-vis spectroscopy was hypothesized to be an

efficient method of detection for the organic compounds because it provides immediate discernment between the nanomaterial and the organic material in solution.

Experimental methods utilized a small molecule approach to simplify the conditions of the experiments. The organic compounds were selected based on the functionalities represented in humic acid, NOM known to interact with the surface of Ag NPs in aqueous environments (Figure 3). Humic acid is composed of carboxylate, hydroxyl, amine, and thiol functionalities, therefore small organic compounds composed of a central benzene ring and the functionalities of humic acid were used to study the interactions between Ag NPs and organic material. Optimal detection of the small organic compounds was necessary to carry out experiments with Ag NPs. To enhance detection of the organic material by UV-vis spectroscopy, pH dependence of the method of detection was studied.

Standard 10 mM solutions of various organic compounds were diluted to 50 µM solutions and pH adjusted, following each pH adjustment UV-vis spectra of the solutions were recorded. Absorbance data produced by pH dependence experiments (Figure 6), shows that at various pH values a shoulder is produced at ~300 nm within the UV-vis spectra of the organic compounds. The production of the shoulder suggests future difficulties quantifying the concentration of the
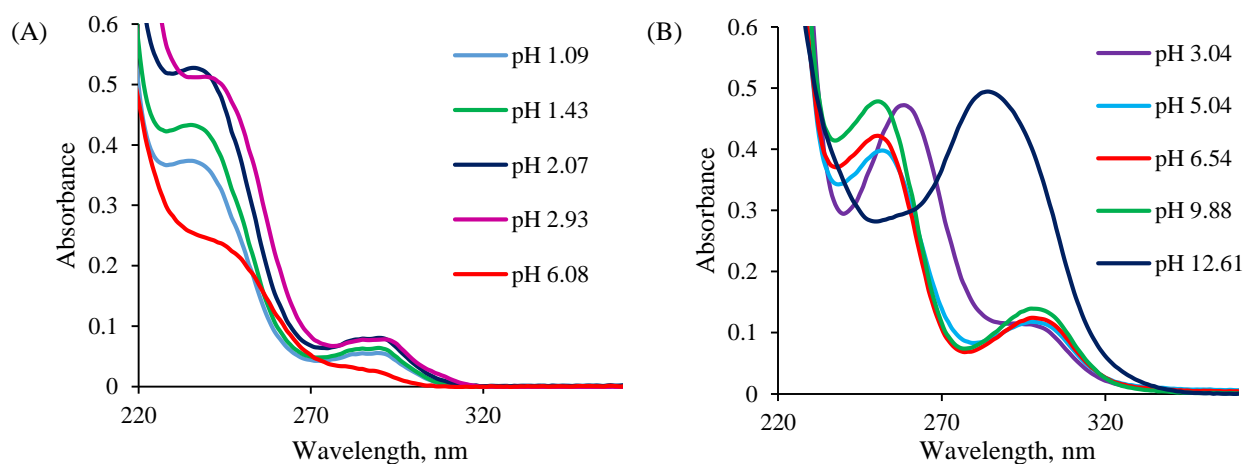

Figure 6. UV-vis spectra of trimellitic acid (A) and 4-hydroxyisophthalic acid (B) at pH values ranging from 1 to 13.

23

material in solution. Therefore, pH ranges in which a single absorbance peak is prominent are considered optimal pH ranges for adsorbate detection.

Preliminary adsorption experiments were carried out using various organic compounds. A known amount of the compound was placed in solution with Ag NPs in a pH 7 MOPs buffer to ensure that experimental conditions were like environmental conditions. After samples were allowed to equilibrate for 2 to 3 hours, the Ag NPs were removed via ultrafiltration. The purpose of the ultrafiltration device was to remove the Ag NPs in solution along with any organic material on their surface, leaving the unadsorbed material in the filtrate. Therefore, by analyzing the filtrate using the UV-vis spectrometer at the pH indicated as the optimal pH in previous experiments, the amount of organic material unadsorbed was quantified using calibration curves. The adsorption could be immediately observed through a decrease in absorbance between the standards and complimentary filtrates (Figure 7A-B). Adsorption experiments in which the concentration of the organic material was increased between samples did not display significant adsorption data when analysis was performed directly after a typical equilibration period (Figure 7A) nor when analysis was performed after an extended equilibration period (Figure 7B). The hypothesized reason for this observation was that there was not enough Ag NP surface area available to produce significant adsorption data. Consequently, the experimental procedure was adjusted to increase the concentration of Ag NPs rather than the organic material.
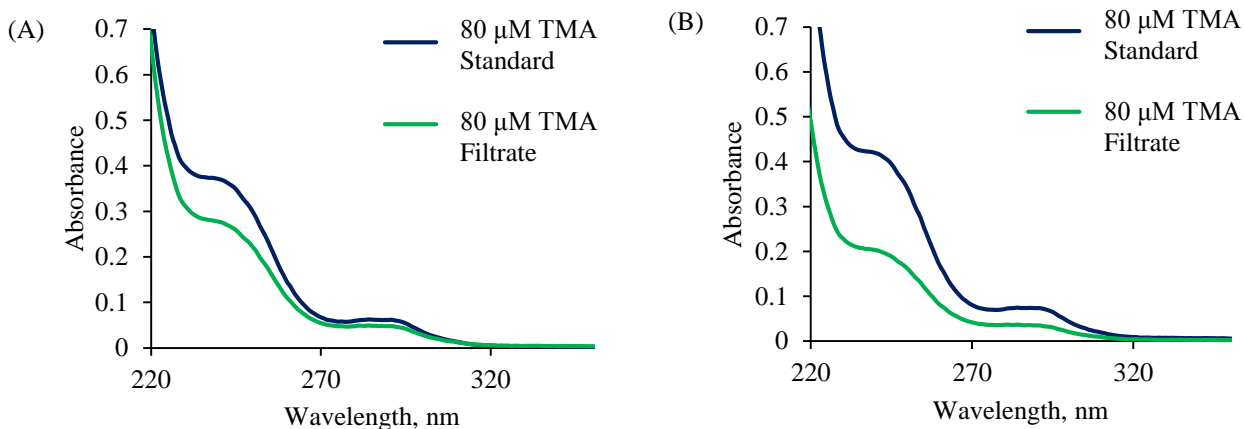
Figure 7. UV-vis spectra of 80 µM trimellitic acid (TMA) standards and filtrates following ultrafiltration of 45 µM Ag NPs and adsorbed material: immediately after sonication (A) and 2.5 hours after sonication (B).

After increasing the concentration of Ag NPs between samples, adsorption of the organic material was still insignificant. The percent of organic material recovered in the filtrate was expected to decrease as the concentration of Ag NPs was increased. The UV-vis data collected showed increases and decreases in the organic material recovered as the concentration of Ag NPs increased between samples (Figure 8). To determine if an extended equilibration period would affect the results, experiments were completed in which samples were given a three-hour and 24-hour equilibration period. The extended equilibration periods were expected to enhance adsorption in solution over time, but data showed that extending equilibration periods resulted in more inconsistent data and less adsorption (Figure 8). Due to insignificant interactions between the organic material and the Ag NPs surface, suspicions rose concerning the capping agent citrate. Capping agents lie on the surface of nanoparticles to deter natural processes like aggregation or dissolution through ionic interactions. Consequently, citrate on the surface of Ag NPs may compete with the organic material in solution to interact with the surface of the Ag NPs. Experiments were carried out in which citrate was "removed" from solution, but the results showed that the citrate content of the samples had no effect on adsorption experimental results.
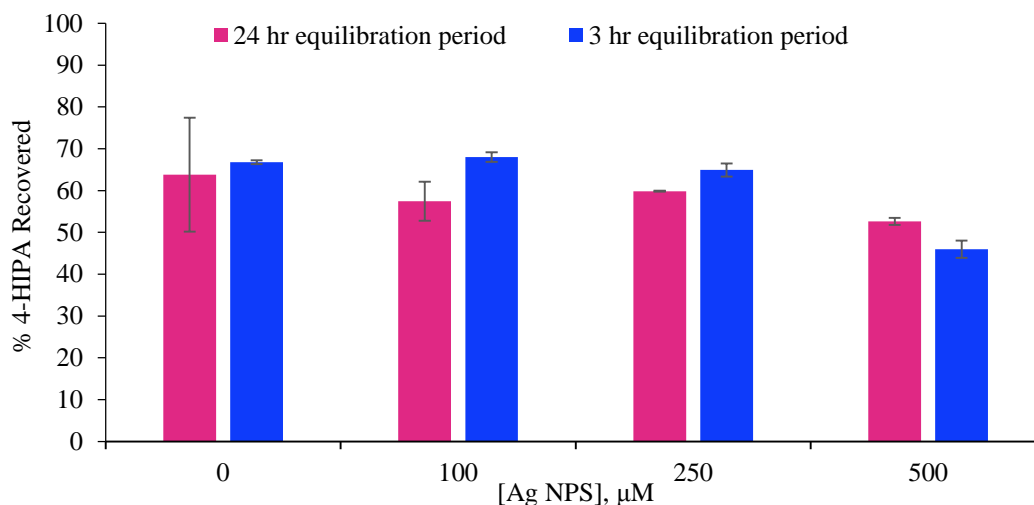
25

Figure 8. Experimental percent recovery results from 4-hydroxyisophthalic acid (4-HIPA) adsorption/ultrafiltration experiment utilizing a three-hour and a twenty-four-hour equilibration period. Error bars represent standard deviation between duplicate samples. (N=2).

To enhance the sensitivity of the detection method and obtain more informative results, High Performance Liquid Chromatography (HPLC) was utilized rather than UV-vis spectroscopy for adsorption/ultrafiltration experiments. As a result of the sensitivity of the detector concentrations utilized to carry out experiments were decreased allowing experiments to be representative of environmental conditions. Experiments in which HLPC was used as a method of detection did not exhibit results in which significant adsorption occurred. In most cases, the percent of organic material recovered resembled the percent of organic material recovered in control samples containing no Ag NPs, indicating no measurable adsorption took place (Figure 9A-C). This was true for organic compounds such as phthalic acid, 4-aminobenzoic acid, salicylic acid, and trimellitic acid. The particularly poor recovery of trimellitic acid was inferred to be a result of electrostatic interactions between the amine and the ultrafiltration device, indicating that separation via ultrafiltration may not be adequate for all adsorbate materials due to differences between the relative pH of the sample solution and the pK_a of the adsorbate material.

Failure to observe measurable adsorption when utilizing functionalities such as carboxylate, amine, and hydroxyl groups led to adsorption/ultrafiltration experiments that focused on the interactions between thiols and the surface of Ag NPs. Though the HPLC was an accurate method for quantification of adsorbate compounds in filtrates following separation from Ag NPs, experiments involving thiols utilized cathodic stripping voltammetry due to the enhanced sensitivity of the instrument in which the thiol may accumulate of the surface of the Hanging Mercury Drop Electrode (HMDE) allowing sub-μM detection. This approach also avoided lengthy thiol derivatization methods that are required for the HPLC analysis of thiols.

Preliminary titration experiments with L-cysteine and Ag NPs showed that there was an interaction between the thiol and the surface of the Ag NPs as the concentration of the thiol decreased as the thiol was titrated with Ag NPs. By repeating the experiment with $AgNO_3$, it was concluded that the interaction previously observed was not due to surface modifications such as aggregation or oxidative dissolution but was due to adsorption.
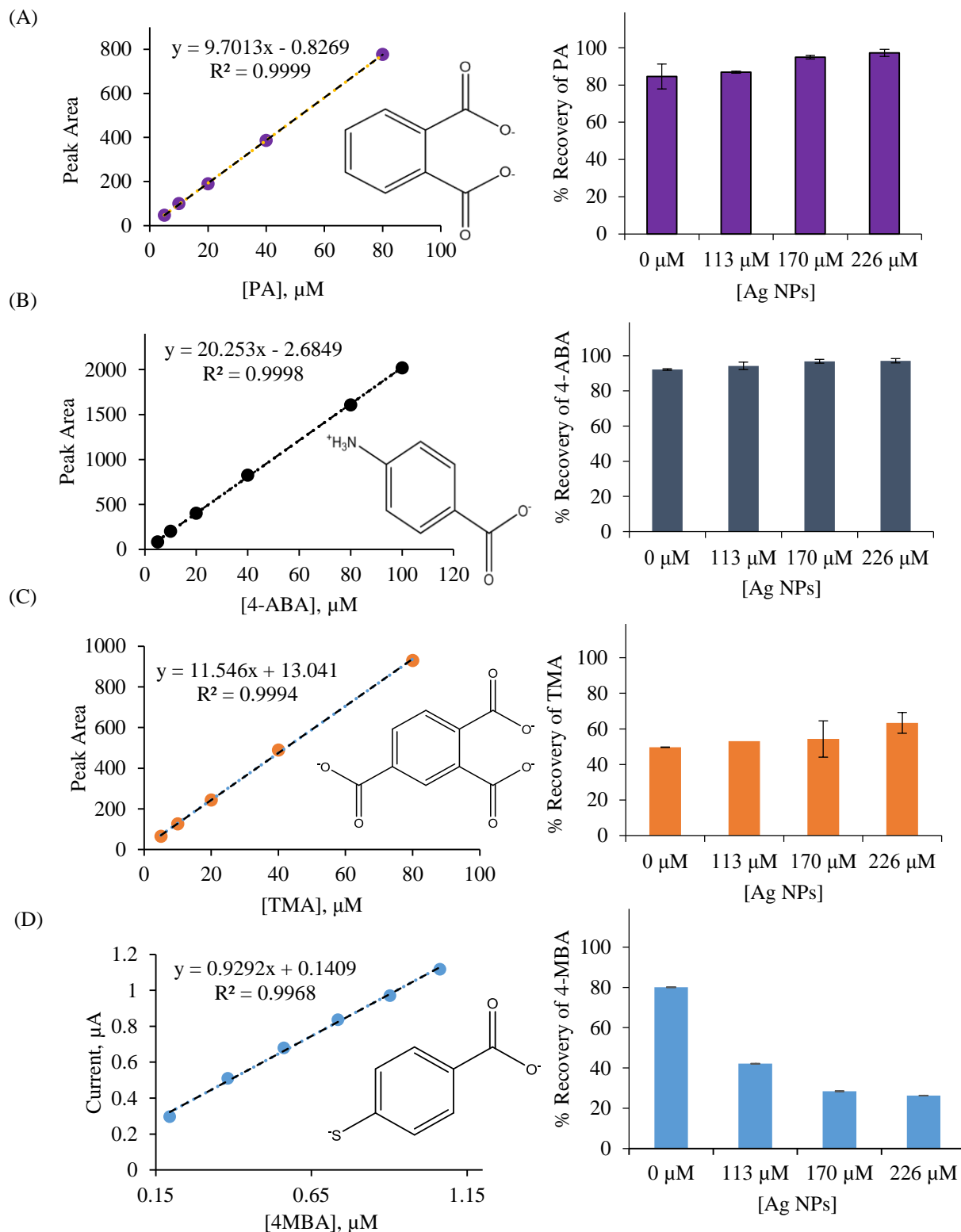
Figure 9. Calibration curves and ultrafiltration/adsorption experiment results for (A) phthalic acid (PA), (B) 4-aminobenzoic acid (4-ABA) and (C) trimellitic acid (TMA) determined by HPLC, as well as (D) 4-mercaptobenzoic acid (4-MBA) determined by voltammetry. Error bars represent standard deviation between duplicate samples. (N=2).

To form a connection between adsorption/ultrafiltration experiments using voltammetry to previous experiments using the HPLC, an adsorption/ultrafiltration experiment in which 4-mercaptobenzoic acid (4-MBA), a thiol, is used was completed using voltammetry. 4-MBA has a similar structure to previously used adsorbate molecules such as 4-hydroxyisophthalic acid, trimellitic acid, and phthalic acid (Figure 9A-C). Results of the ultrafiltration experiment displayed measurable adsorption as the concentration of 4-MBA recovered decreased as the concentration of Ag NPs increased between samples (Figure 9D).

To ensure that the observed results were due to adsorption rather than other surface modifications like aggregation, the UV-vis spectra of Ag NPs alone as well as in a solution with 4-MBA were obtained. The spectra of the solution containing 4-MBA and Ag NPs displayed a red shift representative of aggregation of the nanoparticles in solution (Figure 10A). Aggregation in the sample was suspected to be due to the polydispersity of nanoparticle size within the nanoparticles synthesized in the lab. TEM images of the nanoparticles showed that the Ag NPs synthesized in the lab in solution may be 5 to 100 nm in diameter.[23–]
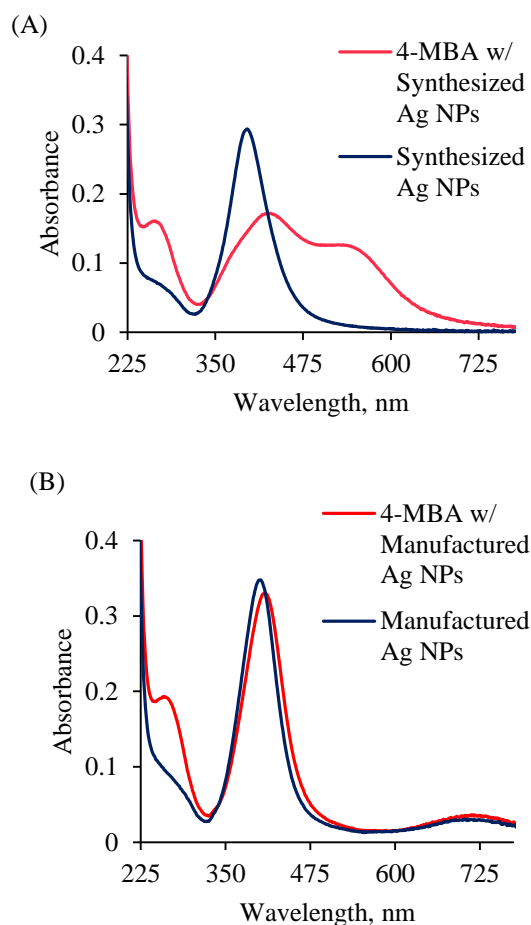
Figure 10. UV-vis spectra of solutions containing Ag NPs synthesized in the lab (A) and 20-nm diameter manufactured Ag NPs (B), along with the Ag NPs in solution with 10 μM 4-mercaptobenzoic acid.

To confirm the cause of the red shift, the UV-vis spectra of manufactured 20-nm diameter Ag NPs alone as well as in solution with 4-MBA were obtained (Figure 10B). The UV-vis spectra did not show the red-shift indicative of aggregation, suggesting that polydispersity of the above-mentioned nanoparticle solution may be the cause of past experimental disparities. Following the aggregation experiment, an adsorption/ultrafiltration experiment was carried out using the manufactured nanoparticles (Figure 11). The results of the experiment showed that measurable adsorption took place in solution as the concentration of adsorbed 4-MBA increased between samples. The adsorption was also greater than the adsorption measured in previous experiments because the enhanced sensitivity of voltammetry allowed experimental concentrations to be lowered an order of magnitude compared to experimental concentrations utilized in previous experiments. Confirmation of adsorption was carried out by titrating 4-MBA with the manufactured Ag NPs and AgNO$_3$ while performing measurements *in situ* using cathodic stripping voltammetry. Silver nitrate proved to immediately interact with 4-MBA by decreasing the concentration of the thiol in solution. As AgNO$_3$ was added to the cell, the concentration of the thiol in solution remained constant following the initial addition of silver but titrating the thiol with
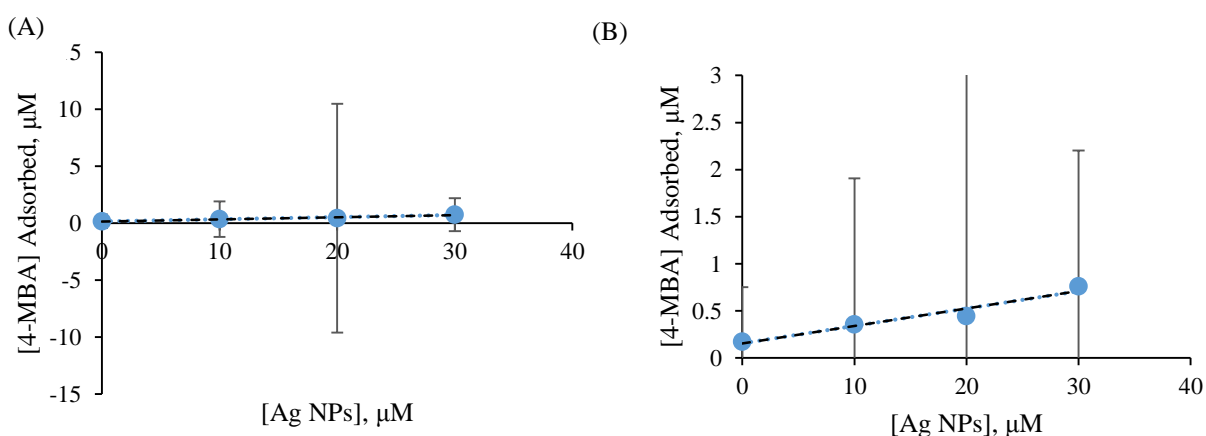

Figure 11. A) Results of adsorption/ultrafiltration experiment in which 20-nm diameter manufactured Ag NPs are placed in aqueous solution with 10 μM 4-mercaptobenzoic acid. Error bars represent standard deviation between results of duplicate samples. (N=2). B) Rescaled results of the adsorption/ultrafiltration experiment.

Ag NPs displayed a similar trend as the adsorption/ultrafiltration experiment in which the concentration of 4-MBA decreased as the nanomaterial was added to the cell of the electrode (Figure 12).
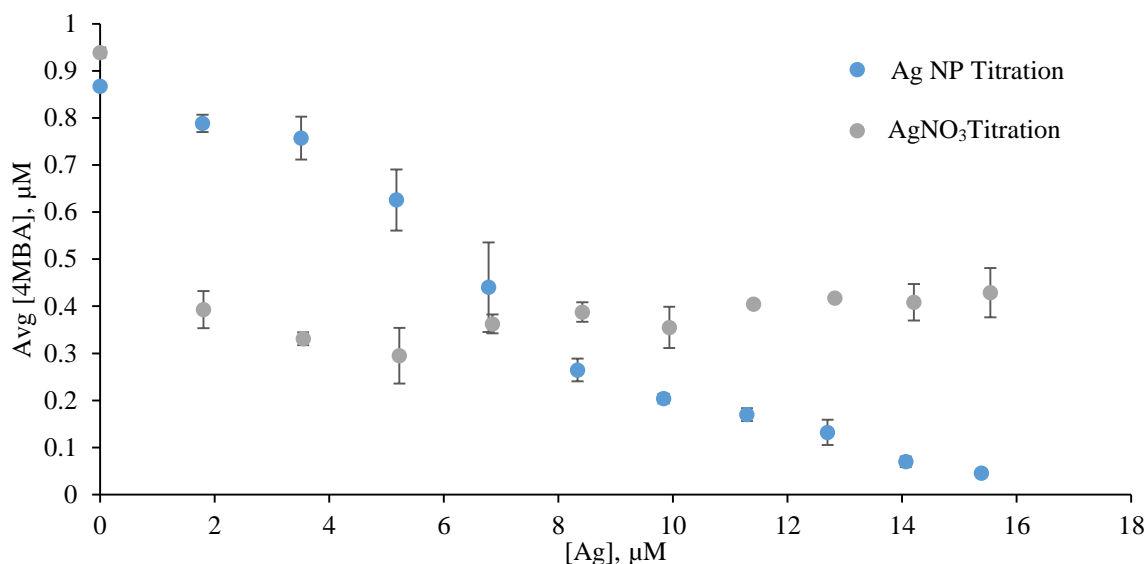

Figure 12. Results of titration experiment performed with manufactures 20-nm Ag NPs and the complimentary experiment performed with silver nitrate utilizing cathodic stripping voltammetry (CSV). Error bars represent standard deviation of triplicate scans. (N=3)

The adsorption/ultrafiltration experiment utilizing 4-MBA and the manufactured nanoparticles was carried out in a pH ~7 MOPs buffer. To compare the interactions between various thiols and Ag NPs, the experiment was repeated with L-cysteine as the adsorbate molecule. When the experiment was carried out in a pH ~7 MOPs buffer, the percent recoveries of L-cysteine as the concentration of Ag NPs increased looked relatively similar to that of the control indicating that no measurable adsorption took place in solution. The pH of the solution was hypothesized to be the cause of the results; therefore, the experiment was repeated in a pH ~8 TRIS buffer. At a pH of ~8, more of the thiol in solution will be deprotonated due to the pK_a of L-cysteine approximately 7.4, making the thiol more available for coordination with the Ag NP surface. This
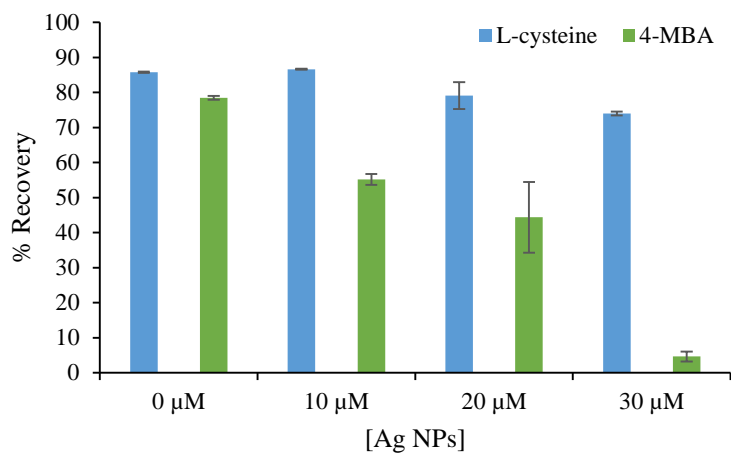
Figure 13. L-cysteine and 4-MBA adsorption/ultrafiltration experimental results using 20-nm diameter Ag NPs. Error bars represent standard deviation between duplicate samples. (N=2).

hypothesis was supported by the experimental results in which the percent recovery of L-cysteine decreased as the concentration of Ag NPs increased between samples. The results also showed that 4-MBA may have a stronger affinity for the surface of Ag NPs because the decrease in the percent recoveries of L-cysteine were not as significant as those of 4-MBA, indicating that conjugation may affect the extent to which adsorption takes place (Figure 13).

The typical limitation with the use of ultrafiltration is electrostatic interactions between the organic material and the filter media during centrifugation. This limitation is evident in the percent recovery of the control sample throughout the experiments discussed thus far; this value typically ranges from 80% to 90% (Figure 14). To reduce the systematic error within this experimental
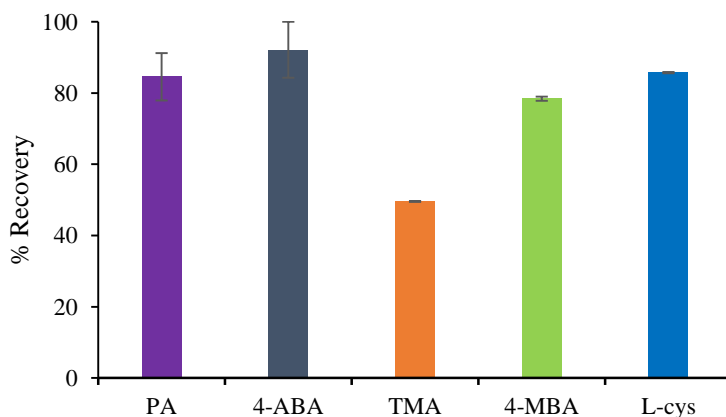
Figure 14. Percent recovery of ultrafiltration/adsorption controls for phthalic acid (PA), 4-aminobenzoic acid (4-ABA), and trimellitic acid (TMA) determined by HPLC, as well as 4-mercaptobenzoic acid (4-MBA) and L-cysteine (L-cys) determined by voltammetry. Error bars represent standard deviation between duplicate samples. (N=2).

design, the ultrafiltration method was abandoned for a centrifugation method in which the experimental nanoparticle solutions are centrifuged at $21,000 \times G$ speed for 30 minutes at $22 \, ^{\circ}C$ following the equilibration of the samples. The centrifugation method effectively removed Ag NPs from unabsorbed

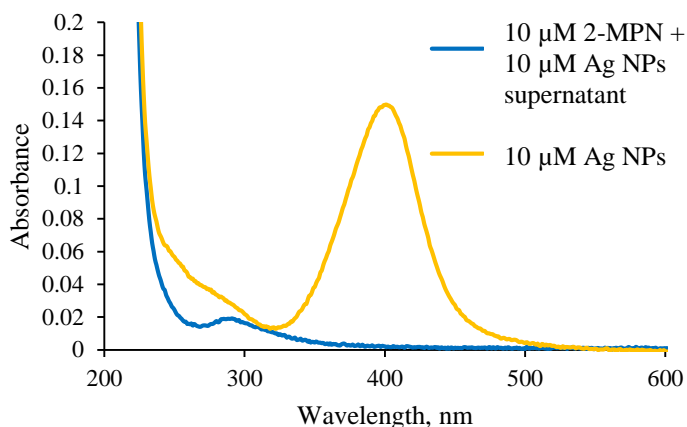**Figure 15.** UV-vis spectra of 10 μM 20-nm Ag NPs and the supernatant resulting from the centrifugation of 10 μM 2-MPN in solution with 10 μM 20-nm Ag NPs in pH ~7 MOPs buffer.

thiol in solution (Figure 15) and exhibited adsorption between experimental samples. The concentration of the adsorbate was increased between samples based promising conclusions drawn from adsorption/ultrafiltration on experiments completed within the lab (Figure 16). Similar adsorption/centrifugation experiments were completed with the thiols based on the significant adsorption of the thiol 4-MBA in previous experiments. The concentration of the adsorbate
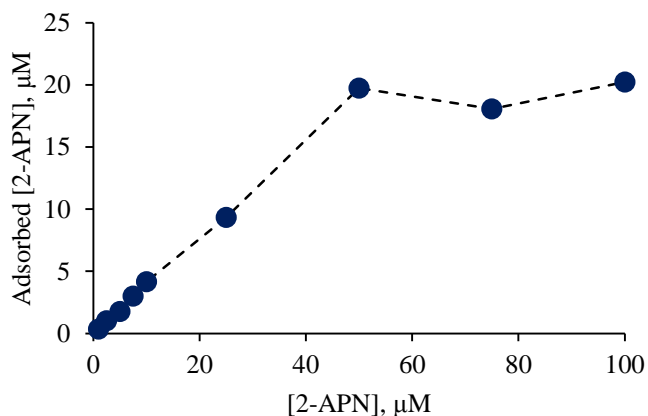

Figure 16. Adsorption/ultrafiltration experimental results carried out with 4-aminophenol (4-APN) and 20-nm diameter Ag NPs increasing the concentration of adsorbate between samples. Experiment performed by Bach Nguyen.

material ranged from 1 μM to 20 μM of thiol in solution, while the concentration of manufactured 20-nm diameter Ag NPs stayed consistent at 10 μM. Adsorption/centrifugation experiments using this sample preparation were successfully completed with 2-mercaptophenol (2-MPN) and 4-aminothiophenol (4-ATP) (Figure 17).

33

The preliminary ultrafiltration experiments carried out with 4-MBA showed surface saturation of the Ag NPs in solution when approximately 10 μM of the adsorbate was bound to the surface of the Ag NPs, but this plateau was not observed in results of centrifugation adsorption experiments. Absence of the
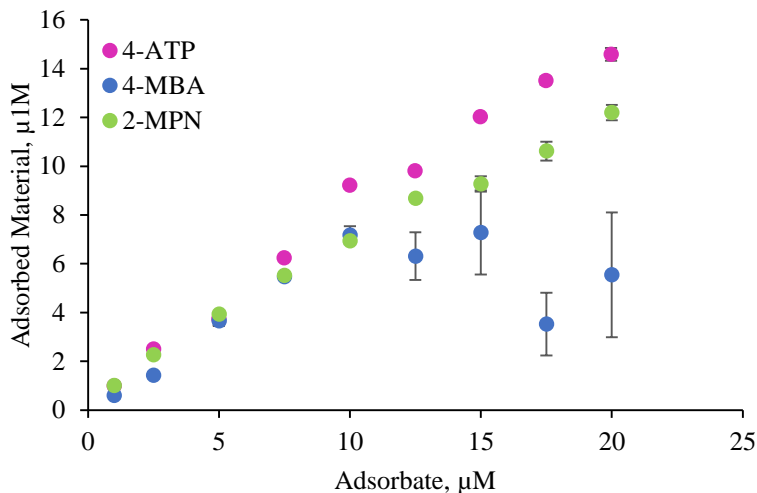

Figure 17. Adsorption/centrifugation experimental results carried out with 4-aminothiophenol (4-ATP), 2-mercaptophenol (2-MPN), and 20-nm diameter Ag NPs increasing the concentration of adsorbate between samples as well as results from a complementary adsorption/ultrafiltration experiment with 4-mercaptobenzoic acid (4-MBA) performed by Bach Nguyen. Error bars represent standard deviation between sequential scans. (N=3).

plateau suggests the formation of a bilayer on the surface of the Ag NPs created by the adsorbate. The ultrafiltration technique possibly removed weakly bound material suggesting surface saturation, while the centrifugation technique offered a more accurate representation of the affinity of the organic material for the Ag NPs surface. Disparities among the results of the thiols confirm the role of organic functionalities in the extent to which adsorption occurs.

Separation via centrifugation was inadequate for the thiol 4-MBA due to interactions at the surface of the NPs such as dissolution. Dissolution studies were completed for 4-MBA, 4-ATP, and 2-MPN in the lab, in which a solution of 10 μM of the adsorbate material was placed in a 10-cm plastic cuvette and spiked with 20-nm Ag NPs to produce a solution of 10 μM Ag NPs. Upon spiking the adsorbate solution with Ag NPs, UV-vis spectra were collected over time. Initially, the peak at approximately 400 nm indicative of Ag NPs decreases because of dissolution. After approximately 1 day, a red shift was observed for the 4-ATP and 2-MPN solutions because of

aggregation (Figure 18A-B). In contrast, no red shift was observed for the 4-MBA solution over the course of 4 days suggesting that dissolution occurred at a greater extent than aggregation in the 4-MBA solution (Figure 18C). Therefore, for separation via centrifugation to be efficient, slight aggregation of the NPs in solution is necessary. Aggregation did not significantly affect adsorption results because as shown through Figures 17 and 18 4-ATP adsorbed to the surface of the Ag NPs to a greater extent than 2-MPN though aggregation was more prevalent in the 4-ATP solution. Furthermore, aggregation of the Ag NPs did not affect adsorption results as significantly as the organic functionalities present. The significant adsorption of 4-ATP onto the surface of Ag NPs may be attributed to the presence of an amine and thiol group in a pH 7 solution rather than simply the deprotonated thiol of an adsorbate such as 2-MPN (Table 1). The presence of a cation in solution may provide further assistance in the exchange of the adsorbate for the citrate capping agent on the surface of the Ag NPs.
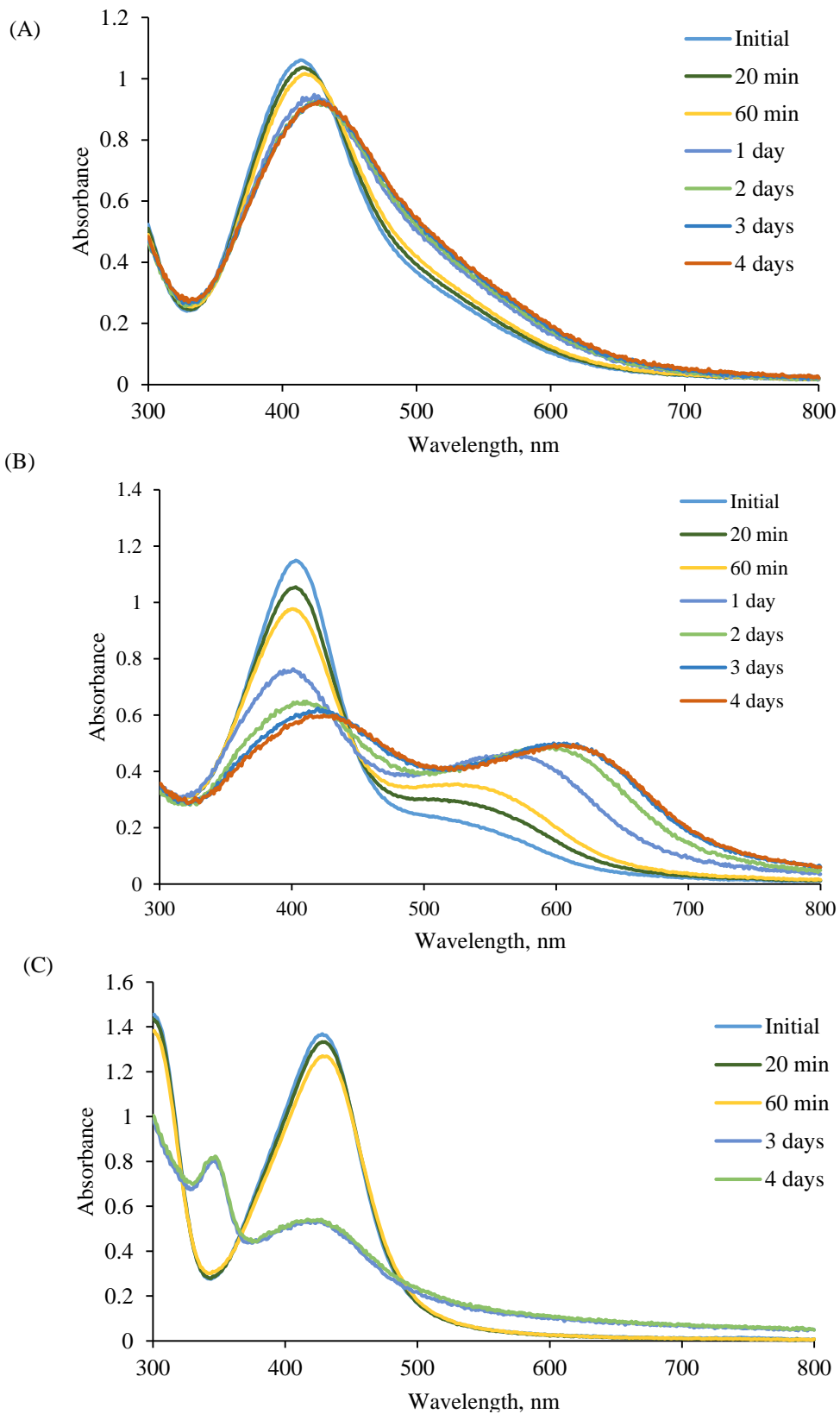
Figure 18. Dissolution study results for 2-mercaptopheno (2-MPN) (A), 4-aminothiophenol (4-ATP) (B), and 4-mercaptobenzoic acid (4-MBA). Experiment performed by Bach Nguyen.

The role of structure of the organic material used during adsorption experiments was also investigated using Surface Enhanced Raman Scattering (SERS). SERS spectra were acquired for solutions of thiol derivatives in combination with Ag NPs. The electromagnetic enhancement due to the presence of silver, produced sharp signals indicative of the functionalities on the surface of the nanoparticles. Signals with the maximum interties were located at approximately 1074 cm^{-1} and 1582 cm^{-1} and were indicative of the aromatic ring of the thiol (Figure 19).[24] The direct correlation between the increase in the concentration of the thiol and the intensity of the signal confirmed adsorption of the thiol onto the surface of the Ag NPs in solution. The spectra also suggest that conjugation plays a significant role in the interactions between natural organic material and Ag NPs in comparison to the organic functionalities of the material by the intensity of the signals representative of the aromatic ring.
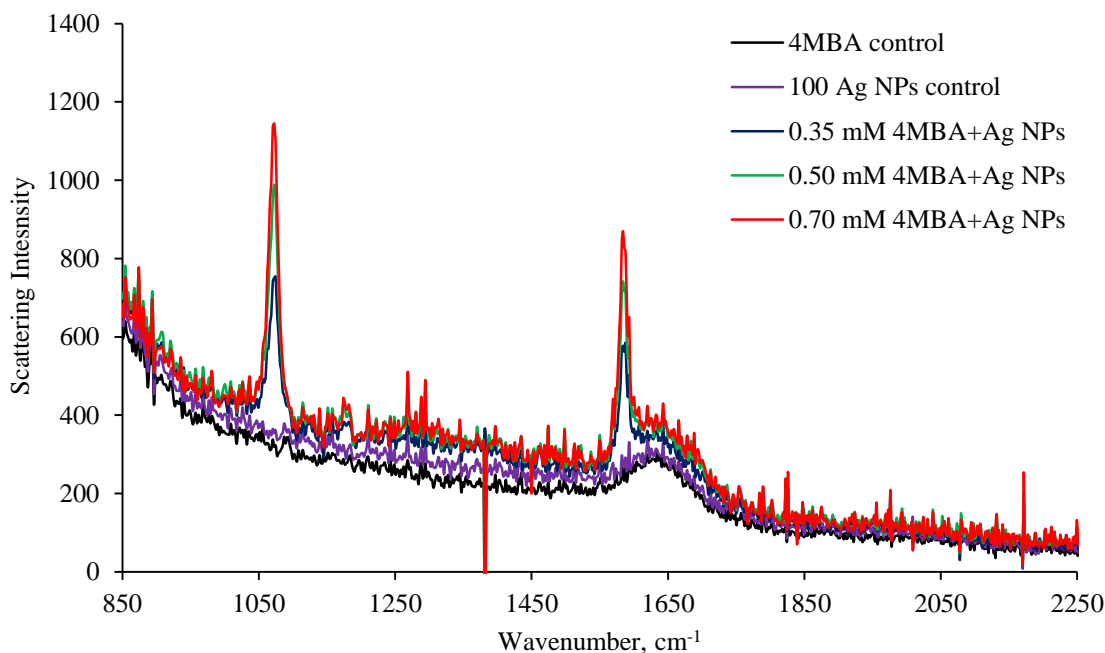

Figure 19. SERS spectra of 4-mercaptobenzoic acid (4-MBA) in solution with manufactured 20-nm diameter Ag NPs with the concentration of the thiol ranging from 0.35 mM to 0.70 mM.

Conclusion

Silver nanoparticles (Ag NPs) are the most commonly used nanomaterial today due to their antimicrobial properties and high reactivity. Research has shown that Ag NPs may interact with natural organic material (NOM) such as humic material in aqueous environments. The interactions between the surface of Ag NPs and NOM may in turn affect the fate of the nanoparticles in aqueous environments. Therefore, the determination of the extent to which these interactions occur is necessary to understand the environmental implications of the increased use in Ag NPs. The research conducted in this report utilized a small molecule approach to conduct adsorption experiments in which the quantity of the adsorbed material was determined utilizing UV-vis spectroscopy, HPLC, and cathodic stripping voltammetry depending on the optimal detection method related to the adsorbate material in use.

Adsorption results varied depending on the pH at which the experiments were carried out, the homogeneity of the NPs in solution, as well as the aromaticity and functionalities of the adsorbate material analyzed. The controlled variables in this laboratory study included pH and the diameter of the Ag NPs in use. Based on the pH of sample solutions, adsorption results varied due to the deprotonation states of the adsorbate molecules being analyzed. Experiments for this environmental study were carried out at a pH of approximately 7 for consistency between experiments. At this pH, the carboxylate and thiol functionalities possibly will be deprotonated to induce complexation reactions between adsorbate molecules and the surface of Ag NPs in solution like those that occur in natural waters. The polydispersity of the Ag NPs solutions prepared in lab resulted in inconsistent adsorption results in initial experiments due to variations in the surface area available as well as the NPs tendency towards aggregation in solution. The use of manufactured 20-nm diameter Ag NPs resulted in adsorption experiments with more reproducible

data due to the monodispersity and increased stability of the NPs in solution. Generally, adsorption results varied based on the adsorbate functionalities present and the structure of the adsorbate molecules.

Adsorption experiments with 4-MBA resulted in relatively significant adsorption of the molecule compared to those with L-cysteine, suggesting that conjugation increases the extent to which adsorption occurs. SERS spectra provided additional support for this conclusion because the most intense Raman signals when 4-MBA and 20-nm diameter Ag NPs were placed in solution were those of the aromatic ring. This is indicative of π–back bonding, in which the π–electrons of the aromatic ring of the adsorbate material are delocalized and available for metal binding.

Experimental results showed that aromatic compounds solely containing carboxylate and hydroxyl functionalities do not have a strong affinity for the surface of Ag NPs compared to those with thiol and amine functional groups. Significant adsorption was observed with 4-mercaptobenzoic acid (4-MBA), 2-mercaptophenol (2-MPN), and 4-aminothiophenol (4-ATP) as well as 4-aminophenol (4-APN). Dissolution studies showed that the adsorption of thiols depended on the other functionalities present as well as their placement near the thiol because the structure of the adsorbate molecule affected the Ag NPs tendency to dissolve or aggregate in solution. These physical transformations affected the efficiency of the separation techniques used; separation via centrifugation was more efficient when adsorbate molecules induced slight aggregation of the NPs in solution. Surface saturation of the Ag NPs in solution was observed through adsorption/ultrafiltration experiments carried out in the lab, but not observed in adsorption/centrifugation experiments suggesting that the use of an ultrafiltration device for separation may disrupt adsorbate bilayers on the surface of the NPs in solution. Therefore,

separation via centrifugation may provide a more realistic view of the interactions at the surface of Ag NPs in natural waters.

Furthermore, physical transformations of Ag NPs in natural waters are influenced by adsorption of NOM onto the surface of the NPs. Additional experiments utilizing separation via centrifugation and large, more conjugated organic molecules will be completed to gain a more comprehensive understanding of the interactions between macromolecular NOM and Ag NPs in natural waters. This methodology may then be applied to other manufactured nanoparticles released into aqueous environments such as ZnO and Cu.

References

1.   Xia, Y. N.; Xiong, Y. J.; Lim, B.; Skrabalak, S. E., Shape-Controlled Synthesis of Metal Nanocrystals: Simple Chemistry Meets Complex Physics? *Angewandte Chemie-International Edition* **2009,** *48* (1), 60-103.

2.   Vance, M. E.; Kuiken, T.; Vejerano, E. P.; McGinnis, S. P.; Hochella, M. F.; Rejeski, D.; Hull, M. S., Nanotechnology in the real world: Redeveloping the nanomaterial consumer products inventory. *Beilstein Journal of Nanotechnology* **2015**, *6*, 1769-1780.

3.   Le Ouay, B.; Stellacci, F., Antibacterial activity of silver nanoparticles: A surface science insight. *Nano Today* **2015**, *10* (3), 339-354.

4.   Quadros, M. E.; Pierson, R.; Tulve, N. S.; Willis, R.; Rogers, K.; Thomas, T. A.; Marr, L. C., Release of Silver from Nanotechnology-Based Consumer Products for Children. *Environmental Science & Technology* **2013**, *47* (15), 8894-8901.

5.   Klaine, S. J.; Alvarez, P. J. J.; Batley, G. E.; Fernandes, T. F.; Handy, R. D.; Lyon, D. Y.; Mahendra, S.; McLaughlin, M. J.; Lead, J. R., Nanomaterials in the environment: Behavior, fate, bioavailability, and effects. *Environmental Toxicology and Chemistry* **2008,** *27* (9), 1825-1851.

6.   Kuhn, M.; Ivleva, N. P.; Klitzke, S.; Niessner, R.; Baumann, T., Investigation of coatings of natural organic matter on silver nanoparticles under environmentally relevant conditions by surface-enhanced Raman scattering. *Science of the Total Environment* **2015,** *535*, 122-130.

7.   Levard, C.; Hotze, E. M.; Lowry, G. V.; Brown, G. E., Environmental Transformations of Silver Nanoparticles: Impact on Stability and Toxicity. *Environmental Science & Technology 2012*, *46* (13), 6900-6914.

8.   Benn, T.; Cavanagh, B.; Hristovski, K.; Posner, J. D.; Westerhoff, P., The Release of Nanosilver from Consumer Products Used in the Home. *Journal of Environmental Quality* **2010**, *39* (6), 1875-1882.

9.   Saleh, N. B.; Das, D.; Plazas-Tuttle, J.; Yang, D.; Del Bonis-O'Donnell, J. T.; Landry, M. P., Importance and challenges of environmental ligand binding and exchange: Introducing single molecule imaging as a model characterization technique. *Nanoimpact* **2017,** *6*, 90-98.

10.   Wang, Z. Y.; Zhang, L.; Zhao, J.; Xing, B. S., Environmental processes and toxicity of metallic nanoparticles in aquatic systems as affected by natural organic matter. *Environmental Science-Nano* **2016**, *3* (2), 240-255.

11.   Delay, M.; Dolt, T.; Woellhaf, A.; Sembritzki, R.; Frimmel, F. H., Interactions and stability of silver nanoparticles in the aqueous phase: Influence of natural organic matter (NOM) and ionic strength. *Journal of Chromatography A* **2011**, *1218* (27), 4206-4212.

12.   Padmos, J. D.; Boudreau, R. T. M.; Weaver, D. F.; Zhang, P., Impact of Protecting Ligands on Surface Structure and Antibacterial Activity of Silver Nanoparticles. *Langmuir* **2015**, *31* (12), 3745-3752.

13.   Laglera, L. M.; Downes, J.; Tovar-Sanchez, A.; Monticelli, D., Cathodic Pseudopolargraphy: A New Tool for the Identification and Quantification of Cysteine, Cystine, and Other Low Molecular Weight Thiols in Seawater. *Analytica Chimica Acta* **2014**, *836*, 24-33.

14.   De Melo, B. A. G.; Motta, F. L.; Santana, M. H. A., Humic acids: Structural Properties and Multiple Functionalities for Novel Technological Developments. *Materials Science & Engineering C-Materials for Biological Applications* **2016**, *62*, 967-974.

15.   Wu, N. J.; Thompson, R., Fast and Efficient Separations Using Reversed Phase Liquid Chromotography. *Journal of Liquid Chromotography & Related Technologies* **2006**, *29*, 949-988.

16.   Fogg, A.G.; Zanoni, M. V. B.; Barros, A. A.; Rodrigues, J. A.; Birch, B. J., Aspeccts of Cathodic Stripping Voltammetry at the Hanging Mercury Drop Electrode and in Non-mercry Disposable Sensors. *Electroanalysis* **2000**, *12* (15), 1227-1232.

17.   Brianina, K. Z.; Malakhova, N. A.; Stozhko, N. Y., Stripping Voltammetry in Environmental and Food Analysis. *Fresenius Journal of Analytical Chemistry* **2000**, *368* (4), 307-325.

18.   Halvorson, R. A.; Vikesland, P. J., Surface-Enhanced Raman Spectroscopy (SERS) for Environmental Analyses. *Environmental Science & Technology* **2010,** *44* (20), 7749-7755.

19.   Yuan, Y. F.; Panwar, N.; Yap, S. H. K.; Wu, Q.; Zeng, S. W.; Xu, J. H.; Tjin, S. C.; Song, J.; Qu, J. L.; Yong, K. T., SERS-based ultrasensitive sensing platform: An insight into design and practical applications. *Coordination Chemistry Reviews* **2017,** *337*, 1-33.

20.   Li, R.; Lv, H. M.; Zhang, X. L.; Liu, P. P.; Chen, L.; Cheng, J. B.; Zhao, B., Vibrational spectroscopy and density functional theory study of 4-mercaptobenzoic acid. *Spectrochimica Acta Part a-Molecular and Biomolecular Spectroscopy* **2015,** *148*, 369-374.

21.   Harris, D. C. *Quantitative Chemical Analysis*; W. H. Freeman and Company: NY 2010; pp AP11-AP19.

22.   Gorham, J. M.; Rohlfing, A.B.; Lippa, K. A.; MacCuspie, R. I.; Hemmati, A.; Holbrook, R. D. Storage Wars: how citrate-capped silver nanoparticles are affected by not-so-trivial decisions. *Journal of Nanoparticle Research* **2014**, *16* (4), 14.

23.   Mullaugh, K. M.; Pearce, O. M. Use of carbon paste electrodes for the voltammetire detection of silver leached from the oxidative dissolution of silver nanoparticles. J*ournal of Nanoparticle Research* **2017**, *19* (4), 1-8.

24.   Kudelski, A. Surface-enhanced Raman scattering study of monolayers formed from mixtures of 4-mercaptobenzoic acid and various aromatic mercapto-derivative bases. *Journal of Raman Spectroscopy* **2009**, *40*, 2037-2043.
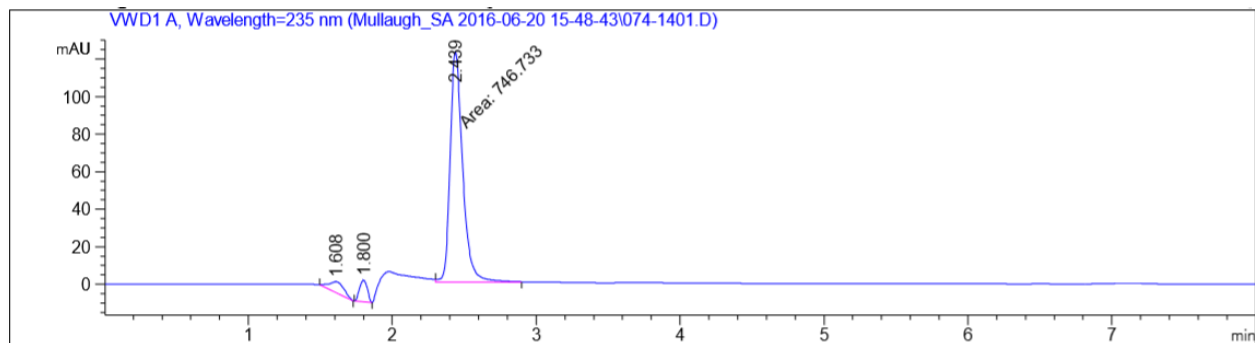
Supplemental Information

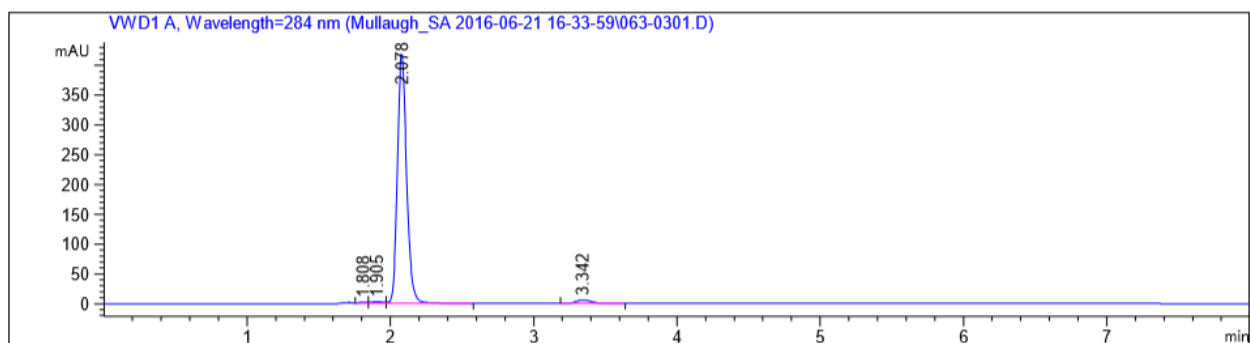Figure S1. Chromatogram of phthalic acid (PA) control.

Figure S2. Chromatogram of 4-aminobenzoic acid (4-ABA) control.
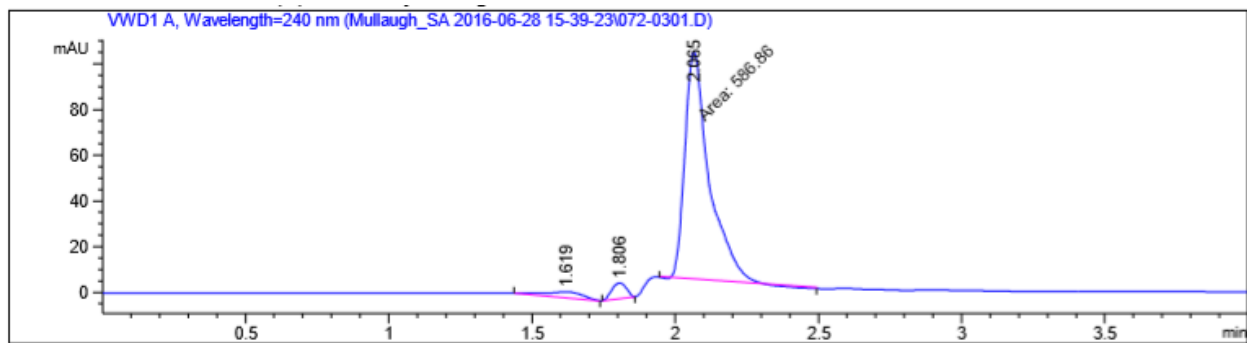

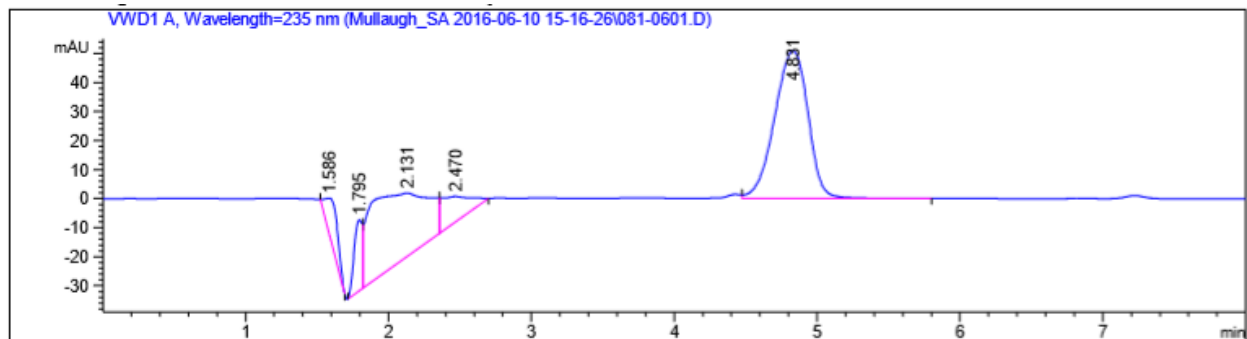Figure S3. Chromatogram of trimellitic acid (TMA) control.

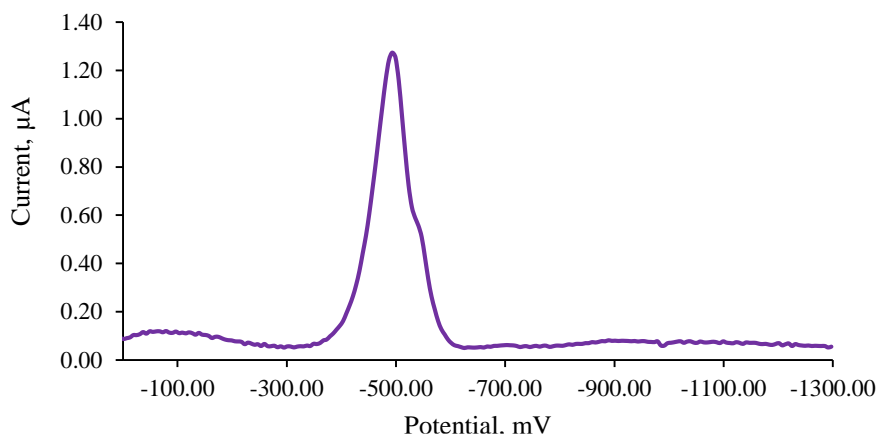Figure S4. Chromatogram of salicylic acid (SA) control.

Figure S5. L-cysteine peak detected by the Hanging Mercury Drop Electrode using cathodic stripping voltammetry.
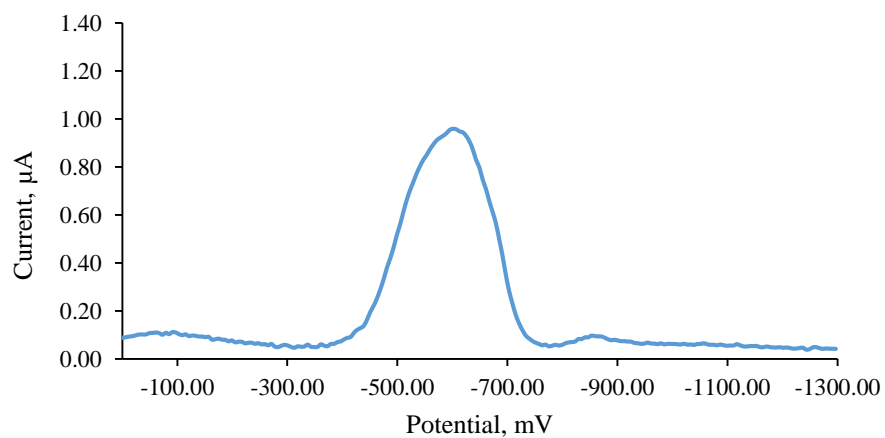

Figure S6. 4-mercaptobenzoic acid (4-MBA) peak detected by the Hanging Mercury Drop Electrode using cathodic stripping voltammetry.
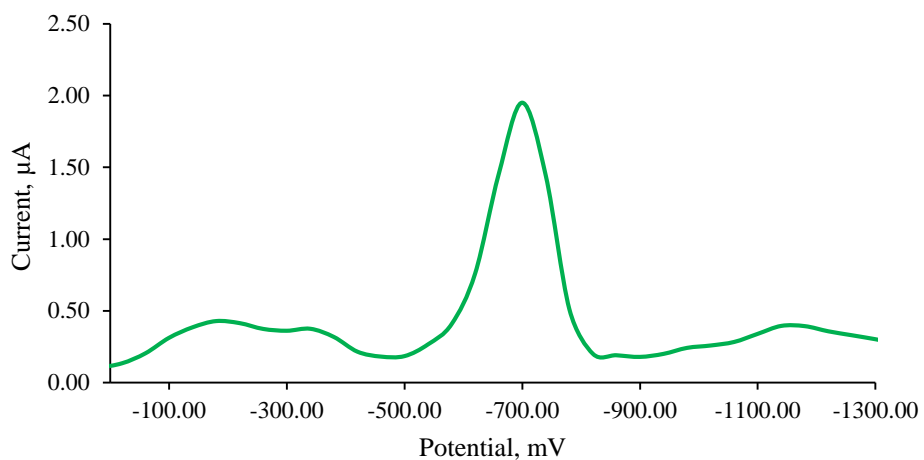
Figure S7. 2-mercaptophenol (2-MPN) peak detected by the Hanging Mercury Drop Electrode using cathodic stripping voltammetry.
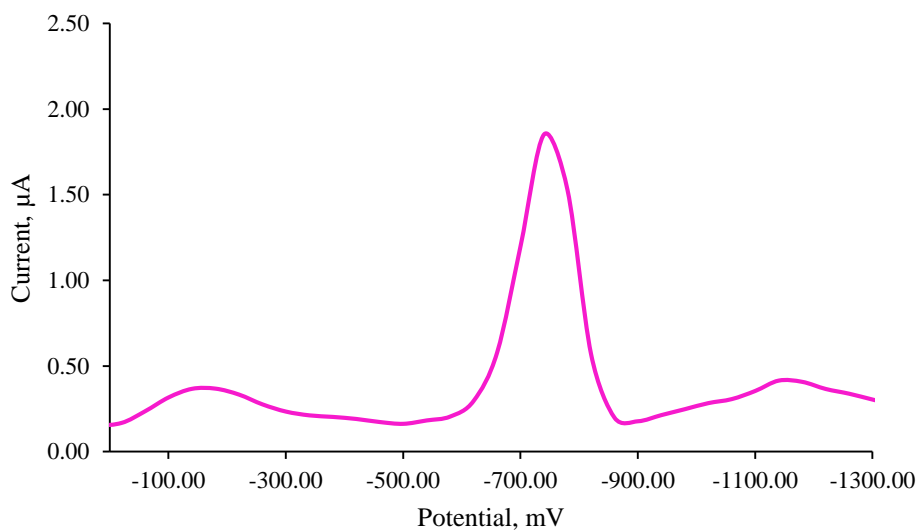

Figure S8. 4-aminothiophenol (4-ATP) peak detected by the Hanging Mercury Drop Electrode using cathodic stripping voltammetry.